,

Does dynamical heterogeneity originate in fluctuations of the time variable?

Karina E. Avila and Horacio E. Castillo*
Department of Physics and Astronomy, Ohio University, Athens, OH, 45701, USA

Azita Parsaeian
Department of Physics and Astronomy, Ohio University, Athens, OH, 45701, USA
and
Materials Research Center, Northwestern University, Evanston, IL 60208-3108, USA

(Dated: July 6, 2010)

Keywords: glass transition, dynamical heterogeneity, structural glass, polymer glass, colloidal glass, granular system, time reparametrization invariance, Goldstone modes, heterogeneous aging

For systems in the vicinity of the glass transition, experiments and simulations have shown the emergence of spatially heterogeneous dynamics (SHD): mesoscopic regions relax either much faster or much slower than neighboring regions [1–8]. SHD is believed to be crucial to the understanding of non-exponential relaxation, the breakdown of the coupling between translational diffusion and viscosity, and even possibly the slowdown of the dynamics itself [1, 2]. The origin of SHD is still uncertain, in part because of the lack of direct microscopic tests to attempt to disprove proposed theories [6, 9–11]. Here we apply one such test [12] for the hypothesis that SHD is associated with fluctuations in the time variable [11, 13, 14], and find that our molecular dynamics data are consistent with the hypothesis. This test can also be applied to particle tracking experimental data in colloidal [4] and granular systems [8], thus allowing to investigate a possible unified explanation of SHD in diverse systems. Our results highlight that non-trivial correlation functions in the time domain contain useful information for the understanding of SHD.

As a glass-forming liquid approaches the glass transition, its relaxation time and viscosity grow by many orders of magnitude, until the system can no longer equilibrate in laboratory timescales, i.e. it has entered the glass state [1]. In equilibrium, the correlation function $C(t, t_w)$ between the states of the system at the *waiting time* t_w and the *final time* t depends only on $t - t_w$, but if the system is out of equilibrium, it may display *aging*, i.e. a nontrivial dependence on both t and t_w. Dynamical heterogeneity can be probed by defining a coarse grained *local* two-time correlation $C_{\mathbf{r}}(t, t_w)$, which will fluctuate in space and time. One of the proposed mechanisms for the origin of dynamical heterogeneity postulates that they are associated with *local fluctuations in the time variable [11, 13–15, 17–19]*. This proposal originated in analytical calculations in spin glass models in the long time limit that showed the presence of a broken symmetry under reparametrizations of the time $t \to h(t)$ [13, 16]. This leads to the prediction of soft modes associated with *local* fluctuations in the time variable [11, 13, 14] $t \to h_{\mathbf{r}}(t)$, i.e.

$$C_{\mathbf{r}}(t, t_w) = C(h_{\mathbf{r}}(t), h_{\mathbf{r}}(t_w)), \tag{1}$$

where $C(t, t_w)$ is the *global* two-time correlation. This is the hypothesis that we test here.

To probe fluctuations in structural glasses, we use [15] $C_{\mathbf{r}}(t, t_w) = \frac{1}{N(B_{\mathbf{r}})} \sum_{\mathbf{r}_j(t_w) \in B_{\mathbf{r}}} \cos(\mathbf{q} \cdot (\mathbf{r}_j(t) - \mathbf{r}_j(t_w)))$. Here $\mathbf{r}_j(t)$ is the position of particle j at time t, $B_{\mathbf{r}}$ denotes a small coarse graining box around the point $\mathbf{r}$, and the sum runs over the $N(B_{\mathbf{r}})$ particles present in the coarse graining box at the waiting time t_w. The *global* correlation function $C(t, t_w) = C_{\text{global}}(t, t_w)$, defined by extending the average to all of the N particles in the system, is the self part of the intermediate scattering function. We have chosen the wavevector $\mathbf{q}$ to be at the main peak of the static structure factor $S(\mathbf{q})$ for the system. We performed classical Molecular Dynamics simulations of systems of N particles ($1000 \leq N \leq 8000$) that were equilibrated at high temperature $T_i >> T_g$, then instantaneously quenched to a final temperature T and allowed to evolve for times several orders of magnitude longer than their typical vibrational times [15, 17–19]. We generated eight datasets by simulating four atomistic glass-forming models: short (10-monomer) polymers interacting via Lennard-Jones (LJ) potentials (dataset A), short polymers interacting via Weeks-Chandler-Andersen (WCA) potentials (dataset B), a binary system of particles interacting via LJ potentials (dataset C), and a binary system of particles interacting via WCA potentials (datasets D-H). The ratio of the final temperature T to the Mode Coupling critical temperature T_c [20] was $T/T_c \sim 0.9$ for datasets A-D, $T/T_c = 1.10$ for datasets

E-F and $T/T_c = 1.52$ for datasets G-H. For datasets F and H, the samples were in equilibrium, but for all the others the samples were aging. Each dataset includes between 100 and 9000 independent runs with the same parameters.

To test the hypothesis given by Eq. (1), we look for a way to probe if a given local fluctuation is due only to a local shift in the time variables. We find two observables $X(t_1, t_2, t_3)$ and $Y(t_1, t_2, t_3)$ such that the *bulk* relaxation trajectory of the system is represented by a *line* in the XY plane. Points along the line correspond to *the same relaxation trajectory* $\{C(t, t')\}_{0 \le t, t' < \infty}$ *at different times*. Points away from the line correspond to a *change in the relaxation trajectory*. We then consider the *local* versions $X_{\mathbf{r}}(t_1, t_2, t_3)$ and $Y_{\mathbf{r}}(t_1, t_2, t_3)$ of the same quantities. If Eq. (1) is true, then those local values should differ from the global ones only by shifts in their time variables, i.e. the points $(X_{\mathbf{r}}(t_1, t_2, t_3), Y_{\mathbf{r}}(t_1, t_2, t_3))$ should fall along the (X, Y) line [12].

To define X and Y, we use the fact that for our data [21]:

$$C(t, t_w) = f\left(\frac{h(t)}{h(t_w)}\right), \tag{2}$$

where f can be fitted as a stretched exponential form as a function of $\theta \equiv \ln(h(t)/h(t_w))$: $f(\theta) = q_{EA} \exp[-(\theta/\theta_0)^\beta]$, with fitting parameters q_{EA}, β and θ_0 that vary little from one dataset to another. However, as the inset in Fig. 1 shows, the dependence of the α relaxation time τ on t_w is quite different in the different systems we consider, and this leads to different forms for $h(t)$ [21]: for aging polymers $h(t) = \exp[\ln^\alpha(t/t_0)]$, for aging particles $h(t) = \exp[(t/t_0)^\alpha]$, and in equilibrium $h(t) = \exp[t/t_0]$.

In order to take advantage of Eq. (2), we define $\Phi_{ab} \equiv f^{-1}[C(t_a, t_b)]$, with $a, b \in \{1, 2, 3\}$ and obtain a *triangular relation* [21]

$$\Phi_{13} = \Phi_{12}\Phi_{23}. \tag{3}$$

This suggests the choices $X \equiv \Phi_{23}/\sqrt{\Phi_{13}}$ and $Y \equiv \Phi_{12}/\sqrt{\Phi_{13}}$, which lead to predict that $1 = XY$ for all times and all systems, as it is indeed found (Fig. 1).

By using Eq. (2), we now reexpress our hypothesis, Eq. (1), in the form

$$C_{\mathbf{r}}(t, t_w) = f\left(\frac{h_{\mathbf{r}}(t)}{h_{\mathbf{r}}(t_w)}\right). \tag{4}$$

If we now define $\Phi_{ab,\mathbf{r}} \equiv f^{-1}[C_{\mathbf{r}}(t_a, t_b)]$, with $a, b \in \{1, 2, 3\}$, $X_{\mathbf{r}}(t_1, t_2, t_3) \equiv \Phi_{23,\mathbf{r}}/\sqrt{\Phi_{13,\mathbf{r}}}$ and $Y_{\mathbf{r}}(t_1, t_2, t_3) \equiv \Phi_{12,\mathbf{r}}/\sqrt{\Phi_{13,\mathbf{r}}}$, we conclude that if the hypothesis in Eq. (1) is satisfied, then $1 = X_{\mathbf{r}}Y_{\mathbf{r}}$, *i.e.* the fluctuating local values of $(X_{\mathbf{r}}, Y_{\mathbf{r}})$ should lie along the same hyperbola as the global values. We thus expect that as the temperature becomes lower, the timescales become longer, and the system becomes more glassy, the probability distribution $\rho(X_{\mathbf{r}}, Y_{\mathbf{r}})$ should become anisotropic, and extend mostly *along* the global curve $1 = XY$ and not *away* from it.

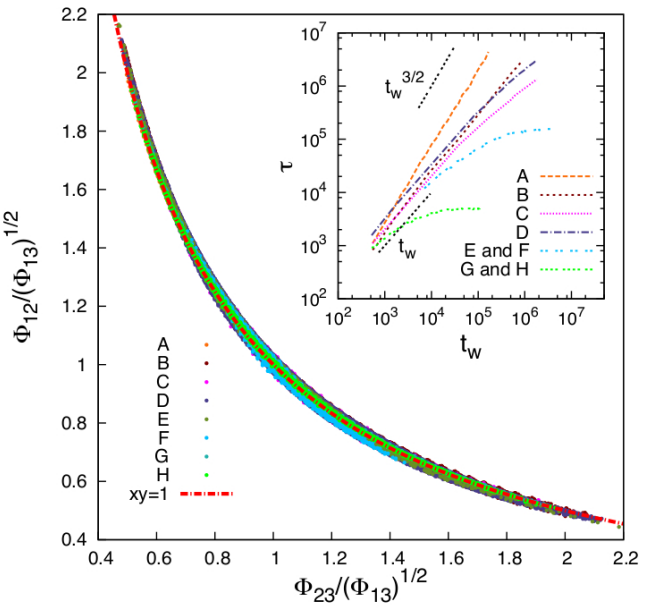

FIG. 1: $(X(t_1, t_2, t_3), Y(t_1, t_2, t_3))$ pairs for all datasets (as labeled in the key) and all possible times $t_1 > t_2 > t_3$. The expected relation $1 = XY$ is shown with a dashed line. *Inset:* Relaxation time τ as a function of the waiting time t_w for all the models and temperatures considered, as identified in the key to the main panel.

In Fig. 2 we show our results for $\rho(X_{\mathbf{r}}, Y_{\mathbf{r}})$. Because we are trying to detect collective fluctuations, we coarse grain over moderately large regions, containing on average 125 particles. For each dataset, we find three triads of times $t_1 > t_2 > t_3$ such that $(X(t_1, t_2, t_3), Y(t_1, t_2, t_3)) \approx (0.8, 1.25), (1.00, 1.00)$, and $(1.25, 0.80)$ respectively. Since time reparametrization symmetry is a long time asymptotic effect, we choose the times as late as possible. For each dataset and time triad, we show three contours of constant probability density $\rho(X_{\mathbf{r}}, Y_{\mathbf{r}})$, respectively enclosing 25%, 50% and 75% of the total probability. For datasets A-D, with $T/T_c \sim 0.9$, the contours indeed follow the curve $1 = XY$. This is more noticeable for the 25% contour, which encloses the most likely fluctuations, than for the 50% and 75% contours, which additionally include rarer events. For datasets E and F, corresponding to $T/T_c = 1.1$, the contours are still anisotropic and oriented along the direction of the global curve, but less so than in A-D, while for G and H, corresponding to $T/T_c = 1.5$ the fluctuations away from the global curve are the strongest. The same trends can be observed in more detail in Fig. 3. This can be directly connected to the fact that, as the

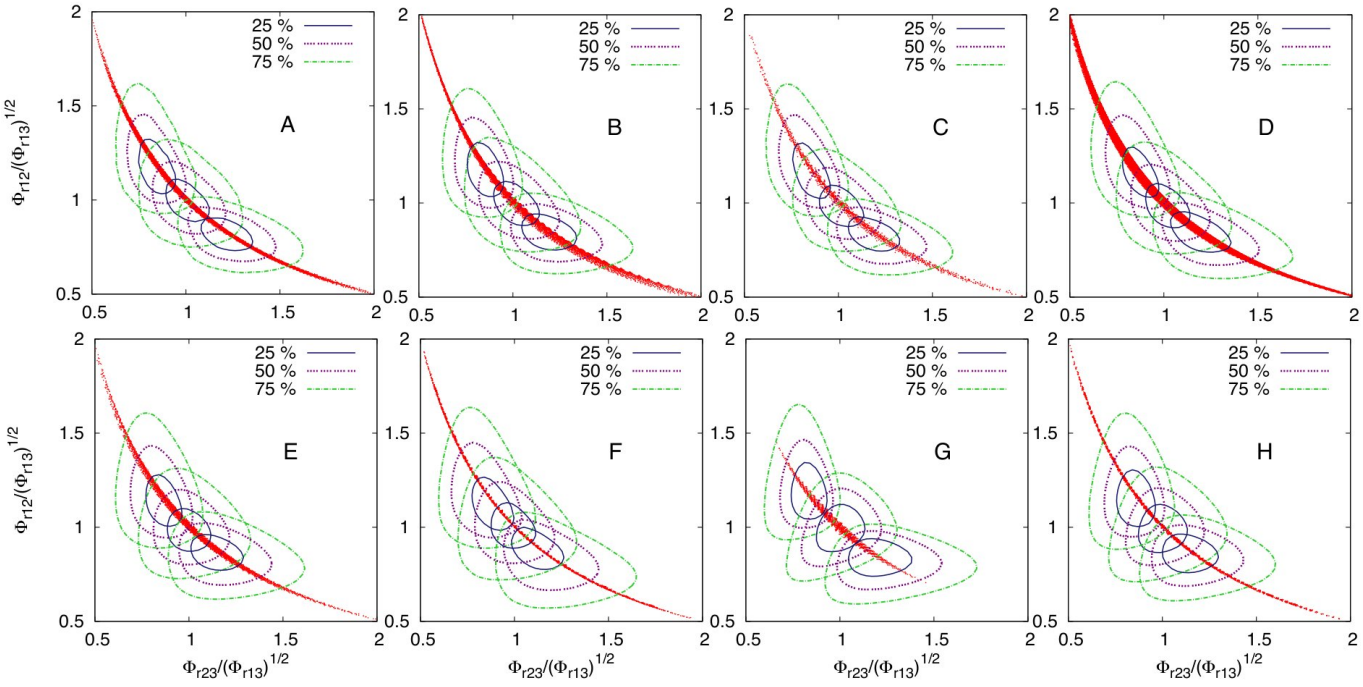

FIG. 2: 2D contours of constant joint probability density $\rho(X_{\mathbf{r}}, Y_{\mathbf{r}}) = \rho(\Phi_{23,\mathbf{r}}/(\Phi_{13,\mathbf{r}})^{1/2}, \Phi_{12,\mathbf{r}}/(\Phi_{13,\mathbf{r}})^{1/2})$, computed using coarse graining boxes containing 125 particles on average. Each set of three concentric contours is chosen so that they enclose 25%, 50% and 75% of the total probability. Each panel from A to H contains results from the corresponding dataset, for $(X, Y) \approx (0.80, 1.25), (1.00, 1.00)$ and $(1.25, 0.80)$, with the times chosen as late as possible within each dataset. The global values $(X(t_1, t_2, t_3), Y(t_1, t_2, t_3))$, for *all* times $t_1 > t_2 > t_3$ in each dataset, are shown with red points.

temperature is increased, the separation of timescales is less pronounced, the finite time corrections to the time reparametrization symmetry become larger, and the effect of local time variable fluctuations become weaker.

For the higher temperatures, we find that the contours obtained in the aging regime (F, H) are similar to the ones obtained in the equilibrium regime (E, G) at the same temperatures [19]. In Fig. 3 we show a contour labeled B', corresponding to the same configurations as for dataset B, but with coarse graining regions containing on average 23 particles. This leads to less averaging and stronger fluctuations, but also, fluctuations with shorter correlation lengths are no longer preferentially supressed, the shape of the contour is no longer dominated by collective modes, and thus contour B' extends dramatically in the direction perpendicular to the global curve. Another contour labeled B" is shown, which corresponds also to dataset B, but with much shorter times. This leads to stronger finite time effects, analogous to the ones found at slightly higher temperatures, and as expected the contour is less anisotropic along the direction of the global curve, and indeed it approaches the contours corresponding to $T/T_c = 1.1$.

Our data also provide evidence for universality [17]: despite the dramatic differences in the dynamics of the four systems A, B, C and D, as illustrated by the inset in Fig. 1, the probability distributions $\rho(X_{\mathbf{r}}, Y_{\mathbf{r}})$ are remarkably similar in the four cases. Together with the fact that in our fits with the form $C(t, t_w) = f\left(\frac{h(t)}{h(t_w)}\right)$ essentially all differences between systems appear in the form of different time reparametrizations $h(t)$, this makes it tempting to speculate that the dynamics of the four models can be approximately mapped into each other just by time reparametrizations, and that these differing time reparametrizations are associated with details of the short time dynamics, but are not essential for the glassy behavior of those systems.

In conclusion, we have applied a stringent microscopic test for the hypothesis that dynamical heterogeneity in structural glasses are associated with the presence of *fluctuations in the time variable*, and we have found that all our results are consistent with this hypothesis. We have used data from molecular dynamics simulations of atomistic systems to apply the test, but the same procedure can be applied to particle tracking data from colloidal [4] and granular systems [8], and slight modifications would allow to study light scattering [7] or dielectric noise [5] data. This opens the door to investigating a possible unified theoretical explanation of dynamical heterogeneity for molecular liquids, colloidal liquids and granular systems. Our results highlight the advantages of studying dynamical heterogeneity by probing fluctuations of

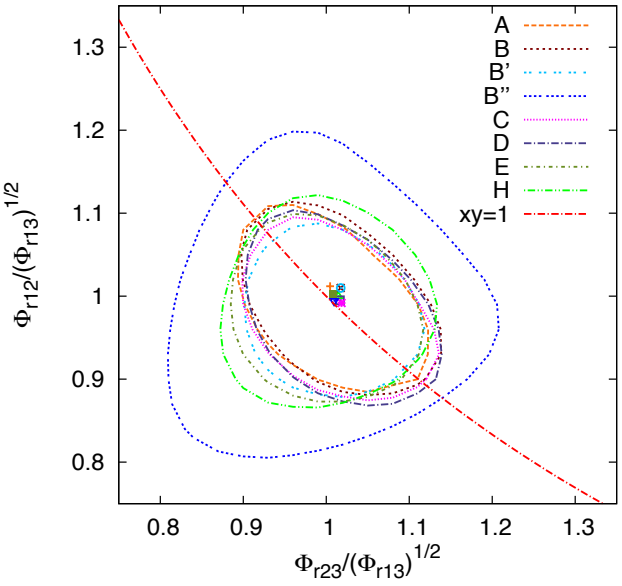

FIG. 3: Comparison of the contours enclosing 25% of the probability for systems A, B, C, D, E and H, where the points near the center of the contours show the global values $\Phi_{23}/(\Phi_{13})^{1/2}, \Phi_{12}/(\Phi_{13})^{1/2}$ for each contour. The contour labeled B' corresponds to the same dataset and times as the one labeled B, but with a much smaller coarse graining size. The contour labeled B" corresponds to the same dataset and coarse graining size and approximately the same global values as the contour labeled B, but with much shorter times

regions of the system, rather than probing *individual particle* fluctuations, since the latter will necessarily contain both collective and non-collective components that are difficult to separate cleanly. They also highlight the fact that more complex correlations in the time domain contain information that is useful for the understanding of heterogeneous dynamical behavior.

H. E. C. thanks L. Cugliandolo and C. Chamon for suggestions and discussions. This work was supported in part by DOE under grant DE-FG02-06ER46300, by NSF under grants PHY99-07949 and PHY05-51164, and by Ohio University. Numerical simulations were carried out at the Ohio Supercomputing Center. H. E. C. acknowledges the hospitality of the Aspen Center for Physics and the Kavli Institute for Theoretical Physics, where parts of this work were performed.

* castillh@ohio.edu

[1] P. G. Debenedetti and F. H. Stillinger, Supercooled liquids and the glass transition. Nature **410**, 259 (2001)
[2] M. D. Ediger, Spatially heterogeneous dynamics in supercooled liquids. Annu. Rev. Phys. Chem. **51**, 99 (2000)
[3] W. Kob, C. Donati, S. J. Plimpton, P. H. Poole, and S. C. Glotzer, Dynamical Heterogeneities in a Supercooled Lennard-Jones Liquid. Phys. Rev. Lett. **79**, 2827 (1997)
[4] E. R. Weeks, L. F. Cugliandolo, A. C. Levitt, A. B. Schofield, and D. A. Weitz, Three-dimensional direct imaging of structural relaxation near the colloidal glass transition. Science **287**, 627 (2000)
[5] E. Vidal Russell and N. E. Israeloff, Direct observation of molecular cooperativity near the glass transition. Nature **408**, 695 (2000)
[6] C. Toninelli, M. Wyart, L. Berthier, G. Biroli, and J.-P. Bouchaud, Dynamical susceptibility of glass formers: Contrasting the predictions of theoretical scenarios. Phys. Rev. E **71**, 041505 (2005)
[7] L. Cipelletti, H. Bissig, V. Trappe, P. Ballesta, and S. Mazoyer, Time-resolved correlation: a new tool for studying temporally heterogeneous dynamics. J. Phys.: Condens. Matter **15**, S257 (2003)
[8] A. S. Keys, A. R. Abate, S. C. Glotzer, and D. J. Durian, Measurement of growing dynamical length scales and prediction of the jamming transition in a granular material, Nature Physics **2007**, 260–264, (2007).
[9] J. P. Garrahan and D. Chandler, Geometrical Explanation and Scaling of Dynamical Heterogeneities in Glass Forming Systems. Phys. Rev. Lett. **89**, 3 (2002)
[10] V. Lubchenko and P. G. Wolynes, Theory of structural glasses and supercooled liquids. Annu. Rev. Phys. Chem. **58**, 235 (2007)
[11] H. E. Castillo, C. Chamon, L. F. Cugliandolo, J. L. Iguain, and M. P. Kennett, Spatially heterogeneous ages in glassy systems. Phys. Rev. B **68**, 134442 (2003)
[12] L. D. C. Jaubert, C. Chamon, L. F. Cugliandolo, and M. Picco, Growing dynamical length, scaling, and heterogeneities in the 3D EdwardsAnderson model J. Stat. Mech. **2007**, P05001, (2007).
[13] C. Chamon, M. P. Kennett, H. E. Castillo, and L. F. Cugliandolo, Separation of Time Scales and Reparametrization Invariance for Aging Systems. Phys. Rev. Lett. **89**, 217201 (2002)
[14] H. E. Castillo, C. Chamon, L. F. Cugliandolo, and M. P. Kennett, Heterogeneous Aging in Spin Glasses. Phys. Rev. Lett. **88**, 237201 (2002)
[15] H. E. Castillo and A. Parsaeian, Local fluctuations in the ageing of a simple structural glass. Nature Physics **3**, 26 (2007)
[16] H. E. Castillo, Time reparametrization symmetry in spin-glass models. Phys. Rev. B **78**, 214430 (2008)
[17] A. Parsaeian and H. E. Castillo, Universal fluctuations in the relaxation of structural glasses. arXiv:0811.3190(2008)
[18] A. Parsaeian and H. E. Castillo, Growth of spatial correlations in the aging of a simple structural glass. Phys. Rev. E **78**, 060105(R) (2008)
[19] A. Parsaeian and H. E. Castillo, Equilibrium and Nonequilibrium Fluctuations in a Glass-Forming Liquid. Phys. Rev. Lett. **102**, 055704 (2009)
[20] U. Bengtzelius, W. Götze, and A. Sjölander, Dynamics of supercooled liquids and the glass transition. J. Phys. C **17**, 5915 (1984)
[21] J.-P. Bouchaud, L. F. Cugliandolo, J. Kurchan, and M. Mézard, Out of equilibrium dynamics in spin-glasses and other glassy systems. arXiv:condmat/9702070(1997)